

10

SPIE.

PROCEEDINGS OF SPIE

VOLUME 9444

INTERNATIONAL SEMINAR ON
**PHOTONICS, OPTICS,
AND ITS APPLICATIONS
(ISPHOA 2014)**

14-15 October 2014
Sanur, Bali, Indonesia

Editor
Aulia Nasution

Organized by
Department of Engineering Physics - FTI
Institut Teknologi Sepuluh Nopember (Indonesia)

Sponsored by
The Optical Society (United States)
PT Telekomunikasi Selular (Indonesia)
PT Len Industri (Indonesia)
PT Sigma Cipta Caraka (Indonesia)

PROCEEDINGS OF SPIE

International Seminar on Photonics, Optics, and Its Applications (ISPhOA 2014)

Aulia Nasution
Editor

14–15 October 2014
Sanur, Bali, Indonesia

Organized by
Department of Engineering Physics – FTI
Institut Teknologi Sepuluh Nopember (Indonesia)

Sponsored by
The Optical Society (United States)
PT Telekomunikasi Selular (Indonesia)
PT Len Industri (Indonesia)
PT Sigma Cipta Caraka (Indonesia)

Published by
SPIE

Volume 9444

10.1117/1.2541111

This document is copyrighted by SPIE. All rights reserved. This document is intended solely for the personal use of the individual user and is not to be disseminated broadly.

The papers included in this volume were part of the technical conference cited on the cover and title page. Papers were selected and subject to review by the editors and conference program committee. Some conference presentations may not be available for publication. The papers published in these proceedings reflect the work and thoughts of the authors and are published herein as submitted. The publisher is not responsible for the validity of the information or for any outcomes resulting from reliance thereon.

Please use the following format to cite material from this book:

Author(s), "Title of Paper," in *International Seminar on Photonics, Optics, and Its Applications (ISPhOA 2014)*, edited by Aulia Nasution, Proceedings of SPIE Vol. 9444 (SPIE, Bellingham, WA, 2015)
Article CID Number.

ISSN: 0277-786X

ISBN: 9781628415599

Published by

SPIE

P.O. Box 10, Bellingham, Washington 98227-0010 USA

Telephone +1 360 676 3290 (Pacific Time) · Fax +1 360 647 1445


SPIE.org

Copyright © 2015, Society of Photo-Optical Instrumentation Engineers.

Copying of material in this book for internal or personal use, or for the internal or personal use of specific clients, beyond the fair use provisions granted by the U.S. Copyright Law is authorized by SPIE subject to payment of copying fees. The Transactional Reporting Service base fee for this volume is \$18.00 per article (or portion thereof), which should be paid directly to the Copyright Clearance Center (CCC), 222 Rosewood Drive, Danvers, MA 01923. Payment may also be made electronically through CCC Online at copyright.com. Other copying for republication, resale, advertising or promotion, or any form of systematic or multiple reproduction of any material in this book is prohibited except with permission in writing from the publisher. The CCC fee code is 0277-786X/15/\$18.00.

Printed in the United States of America.

Publication of record for individual papers is online in the SPIE Digital Library.

SPIE 
Digital Library

SPIDigitalLibrary.org

Paper Numbering: Proceedings of SPIE follow an e-First publication model, with papers published first online and then in print. Papers are published as they are submitted and meet publication criteria. A unique citation identifier (CID) number is assigned to each article at the time of the first publication. Utilization of CIDs allows articles to be fully citable as soon as they are published online, and connects the same identifier to all online, print, and electronic versions of the publication. SPIE uses a six-digit CID article numbering system in which:

- The first four digits correspond to the SPIE volume number.
- The last two digits indicate publication order within the volume using a Base 36 numbering system employing both numerals and letters. These two-number sets start with 00, 01, 02, 03, 04, 05, 06, 07, 08, 09, 0A, 0B ... 0Z, followed by 10-1Z, 20-2Z, etc.

The CID Number appears on each page of the manuscript. The complete citation is used on the first page, and an abbreviated version on subsequent pages.

Contents

- vii *Authors*
- ix *Conference Committee*
- xi *Introduction*
- xiii *Sponsors*

INVITED SESSION

- 9444 02 **Compact one-lens fluorescence microscope using CMOS image sensor (Invited Paper)** [9444-21]
- 9444 03 **Semiconductor lasers for versatile applications from global communications to on-chip interconnects (Invited Paper)** [9444-65]
- 9444 04 **Rigorous characterization of photonic devices by finite element method (Invited Paper)** [9444-66]
- 9444 05 **Photonics engineering: snapshot applications in healthcare, homeland security, agriculture, and industry (Invited Paper)** [9444-67]
- 9444 06 **Identifying the best chalcogenide glass compositions for the application in mid-infrared waveguides (Invited Paper)** [9444-10]

PHOTONICS AND OPTICS APPLICATIONS

- 9444 07 **Large ring laser gyroscopes: towards absolute rotation rate sensing** [9444-62]
- 9444 08 **TOPAS-based humidity insensitive polymer planar Bragg gratings for temperature and multi-axial strain sensing** [9444-19]
- 9444 09 **Activating neurons by light in free-moving adult flies** [9444-4]
- 9444 0A **Liquid level sensing based on laser differential confocal detectors** [9444-16]
- 9444 0B **Evaluating compact SAR polarimetry for tropical forest monitoring** [9444-35]
- 9444 0C **Interferometric processing of C-band SAR data for the improvement of stand age estimation in rubber plantation** [9444-9]
- 9444 0D **Radial line method for rear-view mirror distortion detection** [9444-49]
- 9444 0E **Design of low cost smart infusion device** [9444-43]

- 9444 OF **Tapered fiber optic sensor for potassium detection in distilled water** [9444-60]
- 9444 OG **Web camera as low cost multispectral sensor for quantification of chlorophyll in soybean leaves** [9444-50]
- 9444 OH **Mapping system for the surface temperature in the Ijen Crater by Landsat-8 imagery with supervised image segmentation method based on fuzzy logic** [9444-55]

PHOTONICS MATERIALS

- 9444 OI **Fundamental and harmonic soliton mode-locked erbium-doped fiber laser using single-walled carbon nanotubes embedded in poly (ethylene oxide) film saturable absorber** [9444-26]
- 9444 OJ **Polarization dependent terahertz generation efficiency by optical rectification in LiNbO₃** [9444-31]
- 9444 OK **Al-doped MgZnO/p-AlGaIn heterojunction and their application in ultraviolet photodetectors** [9444-11]
- 9444 OL **Fabrication and characterization of cuprous oxide solar cell with net-shaped counter electrode** [9444-36]
- 9444 OM **The effect of spectrum range limitation to the efficiency of Al_{0.3}Ga_{0.7}As/GaAs/InP/Ge multijunction solar cells: a simulation case** [9444-44]
- 9444 ON **Spectral calibration of the coded aperture spectra imaging system** [9444-8]
- 9444 OO **Co-sensitized natural dyes potentially used to enhance light harvesting capability** [9444-46]
- 9444 OP **Identify paraffin-embedded brain glioma using terahertz pulsed spectroscopy** [9444-32]
- 9444 OQ **Modeling and experiment of dye-sensitized solar cell with vertically aligned ZnO nanorods through chemical bath deposition** [9444-51]
- 9444 OR **Mechanical and optical characterization of bio-nanocomposite from pineapple leaf fiber material for food packaging** [9444-53]

PHOTONICS DEVICE DEVELOPMENTS

- 9444 OS **Fabrication of 1D photonic crystal by sol-gel method for tuning the emission of CdSe colloidal quantum dot** [9444-30]
- 9444 OT **Optical response characteristics of strained uniform fiber Bragg grating using laser diode** [9444-42]
- 9444 OU **Phase matching analyses of anti-Stokes pulses with four wave mixing in birefringence photonic crystal fibers** [9444-37]

- 9444 0V **Using a telecommunication-grade single mode patchcord as an optical extensometer based on bending loss [9444-17]**
- 9444 0W **Load effect on an SMS fiber structure embedded in a high-density polyethylene [9444-58]**
- 9444 0X **Research on key technologies of high repetition rate optical frequency comb [9444-15]**
- 9444 0Y **Optical system design of the snapshot imaging spectrometer using image replication based on Wollaston prism [9444-6]**
- 9444 0Z **Preliminary design of land displacement-optical fiber sensor and analysis of observation during laboratory and field test [9444-18]**
- 9444 10 **SMS fiber structure with a multimode fiber graded index type for a temperature measurement using an intensity-based interrogation system [9444-59]**
- 9444 11 **Design of GaN-based S-bend Y-branch power splitter with MMI structure [9444-41]**
- 9444 12 **16-channel arrayed waveguide grating (AWG) demultiplexer design on SOI wafer for application in CWDM-PON [9444-27]**
- 9444 13 **Broadband millimeter-wave electro-optic modulator using multi patch antennas for pico-cell radar networks [9444-28]**
- 9444 14 **Local density of optical states of an asymmetric waveguide grating at photonic band gap resonant wavelength [9444-5]**

POSTER SESSION

- 9444 15 **A mid-IR optical emission spectrometer with a PbSe array detector for analyzing spectral characteristic of IR flares [9444-29]**
- 9444 16 **Colour harmony of two colour combinations in clothes matching [9444-12]**
- 9444 17 **Development of optical inspection system for detecting malfunctions of digital micromirror device [9444-34]**

The effect of spectrum range limitation to the efficiency of $\text{Al}_{0.3}\text{Ga}_{0.7}\text{As}/\text{GaAs}/\text{InP}/\text{Ge}$ multijunction solar cells : A simulation case

T. Sumaryada^{*a}, E.S. Wahyuni^a, H. Syafutra^a, H. Alatas^a

Theoretical Physics Division at Department of Physics, Bogor Agricultural University (IPB)
Jalan Meranti Kampus IPB Dramaga Bogor 16680, Indonesia

ABSTRACT

Effect of Spectrum Range Limitation (SRL) to the efficiency and performances of multijunction solar cells $\text{Al}_{0.3}\text{Ga}_{0.7}\text{As}/\text{GaAs}/\text{InP}/\text{Ge}$ was investigated using simulation approach. Simulations were done using two different models, first with No Spectrum Range Limitation (NSRL) and the second with SRL. In the first model each subcell material was free to absorb AM1.5G solar radiation spectrum from 280 nm up to 2500 nm, while for the second model, absorption spectrum for each subcell depends on the cut-off wavelength of its previous subcell. For each model, a identical current flow in each layer was simulated. The results have shown that SRL dropped the efficiency by a half (44.90 %) compared to simulation with NSRL. All current-producing simulations were performed using available PC1D program.

Keywords: Spectrum range limitation, Multijunction solar cells, Simulation, PC1D

1. INTRODUCTION

Solar energy is one of the most promising renewable energy resources in the world. The abundance amount of solar energy and the zero emission produced are some of the reasons that motivate people to continue research in this field. Most of the solar cells available in the market are silicon based panels with efficiency up to 15%, while cheaper panels made from amorphous silicon can only produce half of it [1]. With such a low efficiency a large area will be needed for building a solar farm. As an example the largest solar farm in the world, Topaz solar farm in California, can produce electricity up to 550 MW and power almost 200,000 homes, but it takes about 25 km² area [2]. One way to reduce the area for this massive area is by inventing a new type of solar cells with a high efficiency rate. The development of high efficiency solar cells mostly focused on multijunction solar cells made from III-V compounds like GaAs, AlGaAs, InP, and GaInP. Multijunction solar cells use several semiconducting layers or subcells, each with different bandgap energy and absorption coefficient. Recently some groups have claimed to approach or even surpass 40% solar cells efficiency [5]. Theoretically the more subcells put into, the more electricity produced by the solar cells [6].

Solar energy could also be used to power satellites and outer space vehicles [7]. In outer space we can expect to receive a full blackbody spectrum from the sun, but on the ground the solar energy received is really depend on its position. The reduction of solar energy by the atmosphere is shown by the Air Mass (AM) parameter denoted by $AM = 1/\cos\theta$. As an example, AM0 is the radiation with the orientation angle of 0° (sun is right on top of our head), while AM1.5G is a global solar radiation with the average orientation angle around 48° and the total solar irradiance about 989 W/m². The amount of solar radiated energy will affect the total electrical power produced, so studying the behavior of solar cells under various types and conditions of radiation could benefit us in designing the most efficient solar cells.

In multijunction solar cells, several p-n junction materials were stacked together according to their bandgap energy. The top layer is material with the highest E_g and will absorb solar radiation in the low wavelength region. The next layers are materials with lower E_g and will absorb solar radiation in the higher wavelength regions. In the previous research, we have designed and simulated multijunction solar cells under ideal conditions [8]. In this paper we are interested in comparing the efficiency of multijunction solar cells due to two types of conditions, firstly all materials or subcells absorb the whole solar radiation spectrum (from 280 nm – 2500 nm), and secondly each material absorbs solar

*T. Sumaryada@ipb.ac.id phone +6281219284529

radiation in their respective spectrum range. We will discuss this effect of spectrum range limitation to the perform and efficiency of multijunction solar cells $\text{Al}_{0.3}\text{Ga}_{0.7}\text{As}/\text{GaAs}/\text{InP}/\text{Ge}$ using simulation approach.

2. METHODS

The incident solar radiation to the first subcell was taken from AM1.5G data (ASTM G 173-03) [9], while the off wavelength of each subcell was determined from the coefficient of absorption calculated using Equation (1) [10]

$$\alpha(\lambda) = 5.5\sqrt{(E(\lambda) - E_g)} + 1.5\sqrt{E(\lambda) - (E_g + 0.1)}(\mu\text{m})^{-1}$$

The transmitted intensity to the next subcell $I(\lambda)$ depends on the amount of radiation, thickness of the subcell, an absorption coefficient of the previous subcell (I_0 , d , and $\alpha(\lambda)$), following Equation (2):

$$I(\lambda) = I_0 \cdot e^{-\alpha(\lambda)d}$$

Simulation of power production of each subcell was performed using PC1D program which is developed by Bz *et.al* and freely available in the web [11]. Since this program can only simulate one layer at a time, several simulation must be performed and depending on how many junctions accounted in solar cells. For our simulation (4-junction cells), the total efficiency of solar cells is calculated using:

$$\eta = \frac{P_1 + P_2 + P_3 + P_4}{P_0} \times 100\%$$

Where P_0 is I_0 multiplied by A ($A=1 \text{ cm}^2$, which is the area of solar cell in the simulation) and assumed as the incident solar power to the first subcell, while P_1 , P_2 , P_3 , and P_4 are the output power produced from the subcell number 1, 2, 3, and 4 respectively.

3. RESULTS AND DISCUSSIONS

The profiles of absorbed solar radiation for each model are shown in Figure.1 (a) and (b). For NSRL model each subcell were free to absorb solar radiation within the range of 280 nm to 2500 nm. On the other hand, in SRL model each subcell absorb radiation within a specific range determined by absorption coefficient of the subcell and its previous subcell. For example, GaAs absorbs radiation within the range of 684-873 nm. The value of 684 nm is the cut-off wavelength of the previous subcell ($\text{Al}_{0.3}\text{Ga}_{0.7}\text{As}$), while 873 nm is the cut-off wavelength of GaAs itself. The spectrum range for all subcells were shown in Table.1.

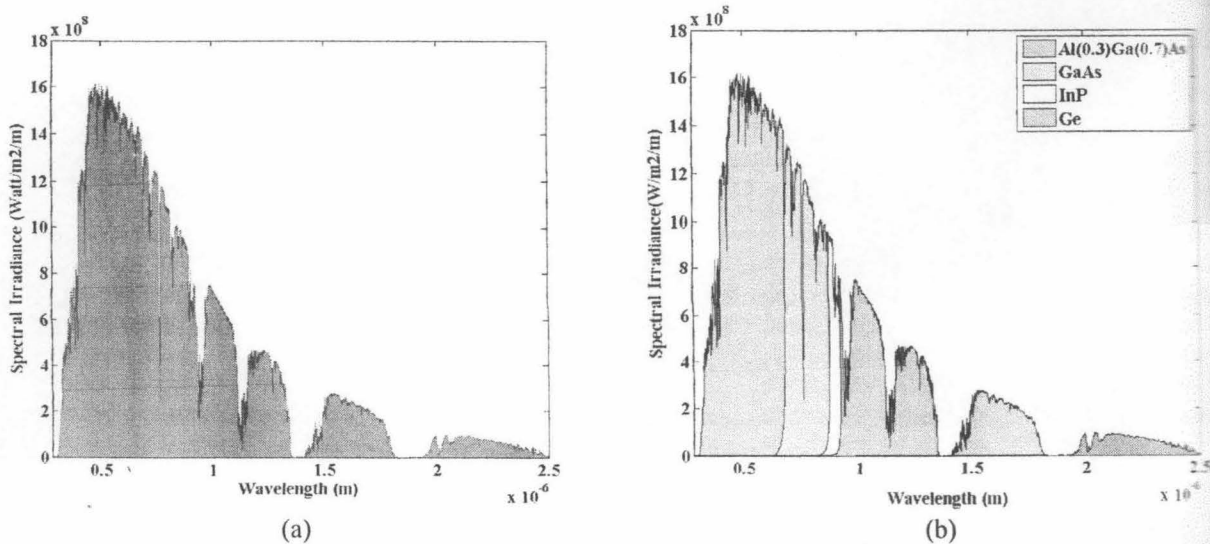
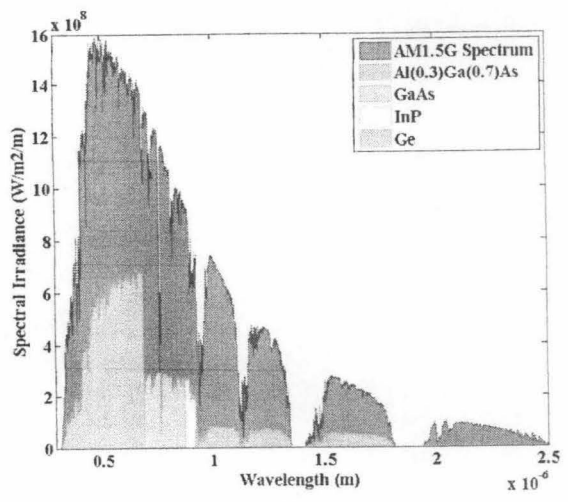
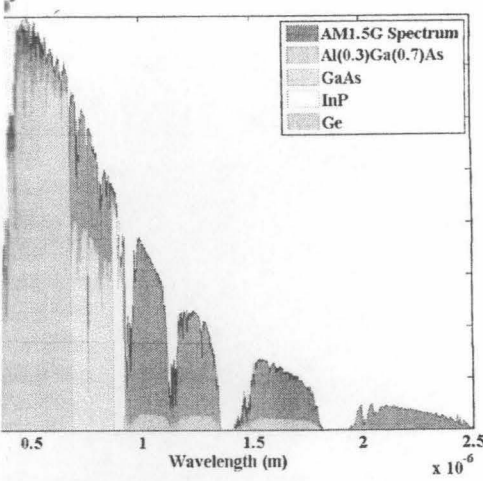


Figure.1 (a) AM1.5G spectrum and the absorption region for each subcell based on NSRL (No Spectrum Range Limitation), and (b) AM1.5G spectrum and the absorption region for each subcell based on SRL (Spectrum Range Limitation).



a) The profile of radiation converted into electricity for each subcell based on NSRL (No Spectrum Range Limitation), and profile of radiation converted into electricity for each subcell based on SRL (Spectrum Range Limitation).

amount of radiation converted into electricity for each subcell can be seen in Figure 2 and Table.1. For Al_{0.3}Ga_{0.7}As, the output electric power produced is 438 mW under NSRL condition, and 198 mW under SRL. This is a 54.79 % drop of efficiency. The amount of radiation loss (radiation which is not being absorbed and not converted into electricity) is defined as the difference between absorbed radiation and the output power. Radiation loss for the first subcell is 10.8 mW (or 2.41 % loss) in NSRL, and 253.8 mW (56.17 % loss) in SRL model. For the second subcell, GaAs, the output power is 130 mW for NSRL and 81 mW for SRL, or a 37.7 % drop of output power. Radiation loss for the second subcell is 76 mW (36.9 % loss) for NSRL, and 122 mW (60.1 % loss) for SRL model. The third subcell, InP, produced 36 mW output in NSRL model, but only 7.6 mW in SRL, or 78.9 % drop of output power. Radiation loss for InP is 3.0 mW (7.69 % loss) for NSRL, and 32.4 mW (81 % loss) for SRL model. The last subcell, Ge, produced 31.6 mW of electricity in NSRL, and 63.6 mW in SRL model. Interestingly, instead of a drop, we gain an increase of efficiency about 101.26 % for this subcell. Radiation loss for Ge is 228.4 mW (87.85 % loss) for NSRL and 164.4 mW (75.8 % loss) for SRL model.

Table 1 Simulation Results.

Type of radiation	Subcell	Incoming radiation (mW/cm ²)	Absorbed radiation (mW/cm ²)	Output Power (mW)	Absorption spectrum range (nm)	Total efficiency (%)
NSRL	Al _{0.3} Ga _{0.7} As	989.80	448.80	438.00	280-2500	64.21
	GaAs	541.00	206.00	130.00	280-2500	
	InP	335.00	39.00	36.00	280-2500	
	Ge	296.00	260.00	31.60	280-2500	
SRL	Al _{0.3} Ga _{0.7} As	989.80	451.80	198.00	280-684	35.38
	GaAs	538.00	203.00	81.00	684-873	
	InP	335.00	40.00	7.60	873-921	
	Ge	295.00	263.00	63.60	921-1864	

From the analysis above, the third subcell, InP, contribute the least to the total efficiency of solar cells. Too much radiation loss, and too little output power produced by InP, especially in SRL model. This problem is probably related to the crystal properties of InP. The lattice constant of $Al_{0.3}Ga_{0.7}As$, GaAs, and Ge are almost identical, about 5.65 Angstrom, while for InP is around 5.90 Angstrom. As we know, lattice mismatch between two adjacent subcells can lead to a significant loss or dissipation of energy during the current producing process inside the solar cells [12,13]. We hypothesize that if we remove InP subcell, and keep the triple junction intact ($Al_{0.3}Ga_{0.7}As/GaAs/Ge$), a better efficiency and minimal radiation loss can be achieved.

There are two ways to model the performance of a multijunction solar cells, first by using non identical currents, and second by using an identical current flow in each subcell. The first is rather unrealistic and unpractical, since in reality we do not harvest the output from each subcell individually. The more realistic way to extract the electric power from solar cells is by forcing the same value of currents flow in each subcell (or setting a series connection of subcells) [8]. In this simulation, we only consider non identical currents flow in each subcell, which is unrealistic, but since we only interested in studying the solar cells behavior under different spectrum range, the same behavior is expected to appear in an identical current model.

The current-voltage characteristic of each subcell under NSRL and SRL condition can be seen in Figure.3. In general we can state that the limitation of spectrum range will drop the values of current (I_{sc}), voltage (V_{oc}), and output power of solar cells.

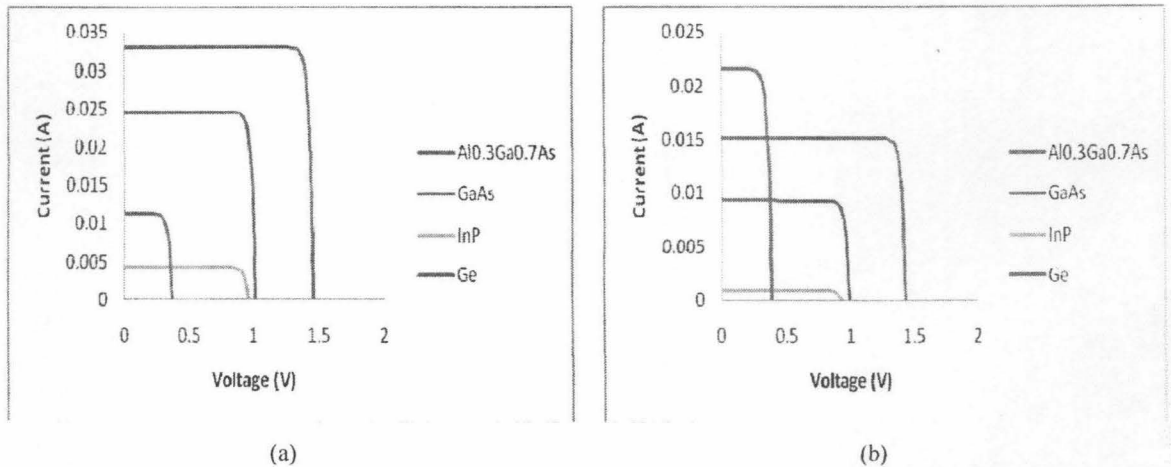


Figure.3 (a) The current-voltage characteristic of each subcell based on NSRL (No Spectrum Range Limitation) model and (b) The current-voltage characteristic of each subcell based on SRL (Spectrum Range Limitation) model.

4. CONCLUSIONS

We have simulated the performance of $Al_{0.3}Ga_{0.7}As/GaAs/InP/Ge$ multijunction solar cells under two types of radiation spectrum, NSRL and SRL. The limitation of spectrum range in each subcell have dropped the total efficiency of solar cells from 64.21 % to 35.38 % . This significant drop (44.90 %) of solar cells efficiency probably due to the lattice mismatch between InP and its neighboring subcells (GaAs and Ge). This lattice mismatch could act as a source of dissipation of power and radiation loss. Removing InP subcell would probably increase the efficiency and reduce the radiation loss in solar cells.

5. ACKNOWLEDGEMENT

Authors express their gratitude to Directorate of Higher Education, Department of Education and Culture Republic of Indonesia for funding this research through 2014 Competitive Grant (HIKOM 2014).

REFERENCES

- Chopra, K.L., Paulson, P.D., Dutta, V., "Thin film solar cells: An overview", *Progress in Photovoltaics: Research and Application* 12, 69-92 (2004).
- Topaz Solar Farm, http://en.wikipedia.org/wiki/Topaz_Solar_Farm.
- Yamaguchi, M., Takamoto, T., Arak, K., Ekins-Daukes, N., "Multijunction III-V solar cells: current status and future potential". *Solar Energy* 79(1), 78-85 (2005).
- King, R. R., Law, D.C., Edmonson, K.M., Fetzer, C.M., Kinsey, G.S., Yoon, H., Sherif, R.A., Karam, N.H., "40% efficient metamorphic GaInP/GaInAs/Ge multijunction solar cells", *Appl. Phys. Lett.* 90, 183516 (2007).
- Yamaguchi, Masafumi, Nishimura, Ken-Ichi, Sasaki, Takuo, Suzuki, Hidetoshi, Arafune, Kouji, Kojima, Nobuaki, Ohsita, Yoshio, Okada, Yoshitaka, Yamamoto, Akio, Takamoto, Tatsuya, Araki, Kenji, "Novel materials for high-efficiency III-V multi-junction solar cells", *Solar Energy* 82, 173-180 (2008).
- Tobías, I., Luque, A., "Ideal efficiency of monolithic, series-connected multijunction solar cells", *Progress in Photovoltaics: Research and Applications* 10 (5), 323-329 (2002).
- Torchynska, T.V., Polupan, G., "High efficiency solar cell for space application", *Superficies Vacio* 17, 21-25 (2004).
- Sumaryada, T., Sobirin, R., Syafutra, H., "Ideal simulation of $Al_{0.3}Ga_{0.7}As/InP/Ge$ multijunction solar cells", *AIP Conf. Proc.* 1554, 162-165 (2013).
- ASTM G173-03 Reference Spectra. <http://rredc.nrel.gov/solar/spectra/am1.5/ASTMG173/ASTMG173.html>
- Olson, M., Friedman, D.J., Kurtz, S., [High-Efficiency III-V Multijunction Solar Cells, in *Handbook of Photovoltaic Science and Engineering*, edited by A. Luque], John Wiley & Sons, Chichester, West Sussex, United Kingdom, 359-411 (2003).
- Basore, P.A., Clugston, D.A., "PC1D Version 5: 32-Bit Solar Cell Modeling on Personal Computers", 26th IEEE Photovoltaic Specialists Conference, Anaheim, 207- 210 (1997).
- Yamaguchi, M., "III-V Compound multi-junction solar cells: present and future", *Solar Energy Materials and Solar Cells*, 75, 261-269 (2003)
- Dimroth, F., "High-efficiency solar cells from III-V compound semiconductors", *Phys. Status Solidi C*, 3: 373-379 (2006).